Published in final edited form as:

FASEB J. 2021 July ; 35(7): e21642. doi:10.1096/fj.202100112R.

Active Rap1-mediated Inhibition of Choroidal Neovascularization Requires Interactions with IQGAP1 in Choroidal Endothelial Cells

Aniket Ramshekar[1], **Haibo Wang**[1], **Eric Kunz**[1], **Christian Pappas**[1,2], **Gregory S. Hageman**[1,2], **Brahim Chaqour**[3], **David B. Sacks**[4], **M. Elizabeth Hartnett**[1,*]

[1]The John A Moran Eye Center, University of Utah, Salt Lake City, UT, USA

[2]Steele Center for Translational Medicine, John A. Moran Eye Center, University of Utah, Salt Lake City, UT, USA

[3]Department of Ophthalmology, Downstate Medical Center, Brooklyn, NY, USA

[4]Department of Laboratory Medicine, National Institutes of Health, Bethesda, MD, USA

Abstract

Neovascular age-related macular degeneration (nAMD) is a leading cause of blindness. The pathophysiology involves activation of choroidal endothelial cells (CECs) to transmigrate the retinal pigment epithelial (RPE) monolayer and form choroidal neovascularization (CNV) in the neural retina. The multidomain GTPase binding protein, IQGAP1, binds active Rac1 and sustains activation of CECs, thereby enabling migration associated with vision-threatening CNV. IQGAP1 also binds the GTPase, Rap1, which when activated reduces Rac1 activation in CECs and CNV. In this study, we tested the hypothesis that active Rap1 binding to IQGAP1 is necessary and sufficient to reduce Rac1 activation in CECs, and CNV. We found that pharmacologic activation of Rap1 or adenoviral transduction of constitutively active Rap1a reduced VEGF-mediated Rac1 activation, migration, and tube formation in CECs. Following pharmacologic activation of Rap1, VEGF-mediated Rac1 activation was reduced in CECs transfected with an IQGAP1 construct that increased active Rap1-IQGAP1 binding but not in CECs transfected with an IQGAP1 construct lacking the Rap1 binding domain. Specific knockout of IQGAP1 in endothelial cells reduced laser-induced CNV and Rac1 activation in CNV lesions, but pharmacologic activation of Rap1 did not further reduce CNV compared to littermate controls. Taken together, our findings provide evidence that active Rap1 binding to the IQ domain of IQGAP1 is sufficient to interfere with active Rac1-mediated CEC activation and CNV formation.

[*]**Correspondence to: M. Elizabeth Hartnett, MD,** Address: 65 Mario Capecchi Drive, Salt Lake City, UT 84132. Tel: 801-213-4110; Fax: 801-581-3357, ME.Hartnett@hsc.utah.edu.

Authors' contributions

AR, HW, and MEH designed the experiments; AR and EK housed the animals; AR, HW, EK, CP performed experiments; AR, HW, and MEH analyzed the data; BC provided *Cdh5*-CreERT2 mice; DBS provided IQGAP1 plasmid constructs; MEH provided funding supports; AR and MEH wrote the manuscript; all authors critically reviewed the manuscript.

Conflicts of Interests

The authors declared there were no conflicts of interests to disclose.

Keywords

Choroidal neovascularization; IQGAP1; Vascular endothelial growth factor; Rac1GTP; Rap1GTP

Introduction

Age-related macular degeneration (AMD) is a leading cause of blindness worldwide[1]. Neovascular AMD (nAMD), an advanced form, accounts for rapid vision loss largely due to the activation of choroidal endothelial cells (CECs) to transmigrate the retinal pigment epithelial (RPE) monolayer and form choroidal neovascularization (CNV) in the neural retina[2,3]. CNV is successfully treated with agents that inhibit the bioactivity of vascular endothelial growth factor (VEGF) but only in approximately 40% of cases[4–6]. Part of this finding may be due to the fact that many factors are involved in the early pathophysiology of nAMD. These include genetic variants, advanced aging, angiogenic factors (e.g., VEGF), inflammatory cytokines (e.g., tumor necrosis factor alpha [TNFα]), and oxidative stimuli (e.g., reactive oxygen species [ROS])[7–11]. We focus on the understudied cellular and molecular events stimulated by external factors that affect signaling cascades that activate CECs, disrupt the integrity of the RPE barrier and lead to CNV. Our long term goal is to improve outcomes in nAMD.

We previously identified Rac1, a Rho GTPase, as a common downstream effector that is activated by several AMD-related stresses, including TNFα[12], VEGF[13,14], and ROS[15]. Rac1 is a biologic switch that is activated by guanine nucleotide exchange factors (GEFs) and inactivated by GTPase activating proteins (GAPs) in response to external stimuli[16]. Rac1 regulates actin polymerization and cell motility when in the GTP-bound (active) state[17–19]. We found Rac1 activation was necessary for CEC transmigration of the RPE[20]. Accordingly, pharmacological inhibition of Rac1 to prevent CEC activation and migration would seem an effective treatment for nAMD, but such a treatment might interfere with the physiologic roles of Rac1GTP[21]. We address this concern by studying mechanisms involved in the pathologic activation of Rac1 in CECs.

We previously reported that pathologic CEC activation and migration required sustained Rac1 activation, which occurred when Rac1GTP bound the GTPase related domain (GRD) of the scaffolding protein, IQ protein motif containing GTPase activating protein (IQGAP1)[14]. IQGAP1 contains other domains in addition to GRD (e.g., calponin homology domain (CHD), poly-proline protein-protein domain (WW), IQ domain, rasGAP-related domain), and each domain binds various proteins that effect different cellular responses[22]. In addition, competitive binding of proteins to one IQGAP1 domain can interfere with binding and activation at another domain, including the GRD[23]. Rap1, a member of the Ras GTPase family, is one protein that can bind the IQ domain of IQGAP1 and interfere with binding of effectors at other domains[24]. We and others found that pharmacologic activation of Rap1 reduced CEC activation[12] and experimental laser-induced CNV in rodents[15,25,26]. In this study, we tested the hypothesis that Rap1GTP binding to IQGAP1 was necessary and sufficient to prevent Rac1GTP-IQGAP1 interactions and reduce pathologic CEC activation and formation of vision-threatening CNV.

Materials and Methods

Choroidal Endothelial Cell Isolation, Genotype, and Culture

CECs were isolated from adult de-identified human donor eyes obtained from the Utah Zions Eye Bank (Salt Lake City, UT) as previously described[14], and were exempt from human subjects research by the University of Utah Investigational Research Board. Genomic DNA was isolated from cultured CECs to genotype for the following AMD-related variants: rs800292 (*CFH* I62V), rs1061170 (*CFH* Y402H), rs1410996 (proxy for protective block), rs12144939 (proxy for *CFHR3/CFHR1* deletion), rs10490924 (*ARMS2* A69S), rs11200638 (*HTRA1* promoter), and rs2230199 (*C3* R102G) through the Steele Center for Macular Degeneration. CECs used in this study all had a low to moderate risk of AMD, which was determined by AMD odds ratios based upon data from over 6,000 case/control individuals[27]. Each experiment used CECs that were obtained from three different donors. Isolated CECs were grown in endothelial growth medium (EGM-2, Lonza, Walkersville, MD) supplemented with 5% fetal bovine serum and were used from passages 3 to 5 for experiments.

Plasmid Transfection, Adenoviral Transduction, and Treatment of Cultured Choroidal Endothelial Cells

CECs were transfected using Lipofectamine 3000 according to the commercial protocol (Life Technologies, Grand Island, NY) with one of the following DNA plasmid constructs: green fluorescent protein (GFP)-tagged full length IQGAP1 (GFP-IQ-WT), GFP-tagged IQGAP1 with the IQ domain deleted (GFP-IQ-ΔIQ)[28], Myc-tagged full length IQGAP1 (Myc-IQ-WT), or Myc-tagged IQGAP1 with selected arginine residues in the third and fourth IQ motifs substituted by glutamine (Myc-IQ-3,4R)[29]. Forty-eight hours after transfection, CECs were serum starved in endothelial basal media (EBM-2, Lonza, Walkersville, MD) for three hours then treated with equal volumes of either 50 ng/mL human recombinant vascular endothelial growth factor (VEGF, R&D Systems, Minneapolis, MN) and 0.05% dimethyl sulfoxide (DMSO), 1 μM 8-(4-chlorophenylthio)adenosine-2-O-Me-cAMP-AM (8CPT-AM; Tocris Bioscience, Minneapolis, MN) and 1 μL PBS, 50 ng/mL VEGF and 1 μM 8CPT, or 1 μL PBS and 0.05% DMSO (vehicle control) for 30 minutes.

CECs were transduced with adenoviral constructs expressing GFP (Ad-GFP) or GFP-tagged constitutively active Rap1a (Ad-GFP-63E) as previously described[12]. Viral vectors were kindly provided by Dr. Keith Burridge (University of North Carolina, Chapel Hill, NC). Forty-eight hours following viral transduction, cells were serum starved for three hours and treated with equal volumes of either 50 ng/mL VEGF or PBS for 30 minutes.

Treatment of non-transfected and non-transduced CECs were performed in similar fashion using doses of VEGF or 8CPT-AM, as indicated in the figures and figure legends.

Immunocytochemistry of Choroidal Endothelial Cells

CECs, grown on glass coverslips (Thomas Scientific, Swedesboro, NJ), were transfected for 48 hours with GFP-tagged IQGAP1 plasmid constructs and then treated with either 1μL PBS and 0.05% DMSO, 50 ng/mL VEGF and 0.05% DMSO, 1 μL PBS and 1 μM 8CPT-AM, or

50 ng/mL VEGF and 1 μM 8CPT-AM for 30 minutes. CECs were fixed for 10 minutes with 4% paraformaldehyde (PFA, Electron Microscopy Sciences, Hatfield, PA) at room temperature and washed three times with PBS. CECs were blocked and permeabilized for one hour at room temperature in PBS containing 5% normal goat serum (NGS) and 0.4% TritonX-100. CECs were stained with rabbit anti-GFP (1:100, Abcam, Cambridge, MA) and either mouse anti-IQGAP1 (1:100, BD Biosciences, San Jose, CA) or mouse anti-Rap1GTP (1:100, NewEast Bioscience, King of Prussia, PA) overnight at 4°C. CECs were washed three times with PBS and incubated for one hour with AlexaFluor 488 goat anti-rabbit secondary antibody (1:500, Abcam, Cambridge, MA) for GFP, AlexaFluor 647-conjugated rat anti-mouse secondary antibody (1:500, BioLegend, San Diego, CA, USA) for IQGAP1 or Cy3-conjugated goat anti-mouse secondary antibody (1:500, Jackson ImmunoResearch Inc., West Grove, PA) for Rap1GTP for one hour at room temperature. After three washes in PBS, the coverslips were mounted in DAPI Fluoromount-G (SouthernBiotech, Birmingham, AL). Images were captured using a confocal microscope (Olympus Corporation, Japan) at 100X objective.

Immunoprecipitation and Western Blots

Following treatment, CECs were washed once with ice cold PBS. Then ice cold radioimmunoprecipitation assay (RIPA) lysis buffer containing both protease inhibitors (Millipore Sigma, Burlington, MA) and phosphatase inhibitors (ThermoFisher Scientific, Rockford, IL) was added to each well. CECs were scraped from the surface of the well plate and transferred to 1.5 mL microcentrifuge Eppendorf tubes. Lysates were clarified by spinning for 10 minutes at 16,000 × *g*, at 4°C. Supernatants were transferred to new Eppendorf tubes, and a bicinchoninic acid (BCA) assay was performed to determine protein concentrations. Protein from cell lysates was suspended in 1X sample buffer and denatured at 95°C for 5 minutes to assess protein expression by western blot. Co-immunoprecipitation (co-IP) or immunoprecipitation (IP) was performed by incubating 400 μg of protein from the same cell lysate with 10 μL Dynabeads protein G (Invitrogen, Carlsbad, CA) and antibodies to either rabbit anti-GFP (1:200, Abcam, Cambridge, MA), mouse anti-Myc (1:50, Santa Cruz Biotechnology, Dallas, Texas), mouse anti-Rac1GTP (1:200, NewEast Bioscience, King of Prussia, PA), or mouse anti-Rap1GTP (1:200, NewEast Bioscience, King of Prussia, PA) overnight with gentle rocking at 4°C. The Dynabead/antibody/protein complex was washed three times with RIPA lysis buffer, re-suspended in 2X sample buffer and denatured at 95°C for 5 minutes. The protein complex bound to GFP, Myc, Rac1GTP, or Rap1GTP was separated by western blot.

Western blots were performed by loading and separating denatured samples in NuPAGE 4% to 12% Bis-Tris Gels (Invitrogen, Carlsbad, CA) followed by transfer to polyvinylidene difluoride (PVDF) membranes (ThermoFisher Scientific, Rockford, IL). PVDF membranes were incubated overnight in 5% bovine serum albumin (BSA) in 1X Tris Buffered Saline (TBS, Quality Biological, Gaithersburg, MD) with one of the following primary antibodies: mouse anti-Rac1 (1:1000, BD Transduction Laboratories, Franklin Lakes, NJ), mouse anti-Rap1 (1:1000, BD Transduction Laboratories, Franklin Lakes, NJ), or rabbit anti-IQGAP1 (1:1000, Abcam, Cambridge, MA). Membranes were washed three times with TBS supplemented with 0.1% Tween-20 (TBST) and then incubated for one hour with

horseradish peroxidase (HRP)-conjugated goat anti-rabbit (1:3000, ThermoFisher Scientific, Rockford, IL) or HRP-conjugated goat anti-mouse (1:3000, Cell Signaling Technology, Danvers, MA) in 5% BSA in 1X TBS. Where indicated, membranes were re-probed with β-actin (1:3000, Santa Cruz Biotechnology, Dallas, Texas) as loading control in 5% milk in 1X TBS.

VEGF and VEGF receptor 2 (VEGFR2) were measured in RPE/choroid tissue lysates using a similar protocol. Briefly, RPE/choroids were sonicated in RIPA lysis buffer and the protein concentration was quantified using a BCA assay. Protein from tissue lysate was suspended in 1X sample buffer and denatured at 95°C for 5 minutes to achieve a final concentration of 1 μg/μL. Western blots were performed, and PVDF membranes were probed with rabbit anti-VEGF (1:500, Santa Cruz Biotechnology, Dallas, Texas) or rabbit anti-VEGFR2 (Cell Signaling Technology, Danvers, MA). PVDF membranes were also re-probed with HRP-conjugated β-actin, as a loading control.

CEC Migration and Tube Formation assays

CEC migration assays were performed as previously described[12,14]. Briefly, thawed Matrigel matrix (Corning, Tewksbury, MA) was diluted with an equal volume of EBM-2 supplemented with either recombinant human VEGF (50 ng/mL) or PBS. Twenty-four well plates were coated with 150 μL of Matrigel mixed with either VEGF or PBS for three hours at room temperature to solidify. 500 μL of EBM-2 was added to each well on top of gelled Matrigel followed by a 6.5 mm diameter Transwell insert (8 μm pores; Corning, NY). CECs stained with Vybrant DiL (Invitrogen, Carlsbad, CA) or transduced with either Ad-GFP or Ad-GFP-63E were seeded on top of the Transwell inserts at 50,000 cells per 100 μL of serum-free EBM-2 media. Vybrant-stained CECs were treated with either 1 μM 8CPT-AM or 0.05% DMSO as vehicle control and incubated for 16 hours at 37°C, 5% CO_2. The migrated CECs on the underside of the Transwell inserts were imaged with a Confocal Laser Scanning Microscope (Olympus Corporation, Japan) at 20X objective. Five different visual fields per Transwell insert were captured. Images were imported into FIJI software, and the number of CECs were quantified.

Tube formation assays were also performed as previously described[14]. Briefly, 45,000 CECs stained with Vybrant DiL or transduced with either Ad-GFP or Ad-GFP-63E were seeded on top of 100 μL of gelled Matrigel in 48 well plates. Vybrant-stained CECs were treated with either 50 ng/mL VEGF and 0.05% DMSO, 1 μM 8CPT-AM and 1 μL PBS, 50 ng/mL VEGF and 1μM 8CPT-AM, or 1 μL PBS and 0.05% DMSO as vehicle control. Transduced CECs by adenovirus were treated with equal volumes of either 50 ng/mL VEGF or PBS. After 12 hours of incubation, tubes were imaged using a Confocal Laser Scanning Microscope (Olympus Corporation, Japan) at 10X objective. Images were imported into FIJI software and the number of tubes were quantified[30].

Animals and Ethical Statement

All animal procedures were approved by Institutional Animal Care and Use Committee, the Institutional Biosafety Committee of the University of Utah and followed the Guide for the Care and Use of Laboratory Animals of the University of Utah and the Association for

Research in Vision and Ophthalmology Statement for the Use of Animals in Ophthalmic and Vision Research. Male and female mice on a C57Bl/6J background were used and routinely tested for *Rd1, Rd8* and *Gnat2* mutations. Genotyping was performed by Transnetyx using real-time PCR. *Iqgap1*$^{tm1A(EUCOMM)Wtsi}$ mice (MGI:5008016) crossed with a *Rosa26Sor*$^{tm1(FLP1)Dym}$ mice (MGI:2429412)[31] were bred to create *Iqgap1*$^{flox/flox}$ mice and crossed with *Rosa26Sor*$^{tm1(EYFP)Cos}$ mice (MGI:2449038)[32] to create *Iqgap1*$^{flox/flox}$;*Rosa26-EYFP*$^{flox/STOP/flox}$ mice (IQ^{fl}). IQ^{fl} crossed with *Cdh5*-Cre/ERT2$^{+/-}$ mice[33,34] were bred to create *Cdh5*-Cre/ERT2$^{+/-}$; *Iqgap1*$^{flox/flox}$;*Rosa26-EYFP*$^{flox/STOP/flox}$ mice (IQ$^{i\Delta EC}$). Four-week-old IQ^{fl} and littermate IQ$^{i\Delta EC}$ received intraperitoneal tamoxifen once every other day (2 mg in corn oil/day) for 3 injections. Mice were anesthetized with intraperitoneal ketamine and xylazine (100 and 10 mg/kg of body weight, respectively) and euthanized by inhalation of isoflurane and subsequent cervical dislocation after confirming they were unresponsive to a toe-pinch.

Laser-induced Choroidal Neovascularization Model and Intravitreal Injections

Six-week-old mice underwent laser-induced choroidal neovascularization (CNV) as previously described[14]. After dilation with 1% tropicamide ophthalmic solution (California Pet Pharmacy, Hayward, CA), anesthetized mice were treated with laser using the Phoenix Image-Guided Laser System 94 (Phoenix Micron IV, Pleasanton, CA) at settings of ~460 mW intensity and 100 ms duration. Generation of cavitation bubbles, indicating disruption of Bruch's membrane, without bleeding was considered successful treatment. Each eye had four laser burns, and each burn was located approximately two-disc diameters from the optic nerve.

Intravitreal injection of either 1 μL of 20.5 μmol/L 8-(4-chlorophenylthio)adenosine-2-O-Me-cAMP (8CPT; Calbiochem, La Jolla, CA) or 1 μL of PBS was administered using a Microliter syringe (Hamilton Company, Reno, NV) as previously described[12,15,26]. Mice received the same treatment in both eyes and were treated with topical erythromycin following injections.

Preparation of RPE/choroids for Flat Mounts, Quantification of CNV volume, and Eyecup Sections

Harvested eyes were corneal clipped and placed in 4% PFA for one hour. Eyes were washed three times with PBS and dissected to isolate the posterior eye cup, which contains RPE/choroid/sclera tissue (herein referred to as RPE/choroid). RPE/choroids were blocked and permeabilized for two hours at room temperature in PBS containing 5% normal goat serum (NGS) and 0.4% TritonX-100, and then stained with AlexaFluor 568-conjugated Isolectin B4 (1:500, Invitrogen, Carlsbad, CA) overnight at 4°C. Radial incisions, avoiding laser lesions, were performed to flat mount RPE/choroids onto a microscope slide with vectashield mounting medium (Vector Laboratories, Burlingame, CA). Confocal z-stack images of each lesion were acquired at 568 nm using a Confocal Laser Scanning Microscope (Olympus Corporation, Japan) at 20X objective. Images were imported into IMARIS (the Oxford Instruments, Switzerland), and CNV volumes were measured using the Surfaces Module (Version 9.1.2, Bitplane, Santa Barbara, California, USA) as previously

described[14,35]. CNV with obvious bridging were excluded from analysis, per standard protocol[36].

For cryosections and immunolabeling, harvested eyes were fixed for one hour in 4% PFA, dissected to remove the extraocular muscle, cornea and lens, and the resulting eyecup washed three times in PBS, then placed into 15% sucrose for three hours and 30% sucrose overnight at 4°C. Eyecups were then embedded in a 2:1 solution of optimal cutting temperature compound (OCT, Sakura Finetek USA, Inc., Torrance, CA, USA):30% sucrose over dry ice. Frozen embedded eyecups were sectioned at 12 μm with a cryostat (Thermo Fisher Scientific, Cheshire, England). Eyecup sections were placed onto charged microscope slides. Sections were washed once with PBS, blocked in 5% NGS in PBS/0.1% TritonX-100 for 1 hour at room temperature, and stained with mouse anti-Rac1GTP (1:100), mouse anti-IQGAP1 (1:100), or rabbit anti-GFP (1:200, Abcam, Cambridge, MA) overnight at 4°C. Sections were washed three times with PBS and incubated for one hour with AlexaFluor 568-conjugated Isolectin B4 (1:500) to label vessels, TO-PRO-3 (1:500, Thermo Fisher Scientific, Waltham, MA) or DAPI to label cell nuclei, and either FITC-conjugated goat anti-mouse secondary antibody (1:500, Invitrogen, Carlsbad, CA) for Rac1GTP, AlexaFluor 647-conjugated rat anti-mouse secondary antibody (1:500, BioLegend, San Diego, CA, USA) for IQGAP1, or AlexaFluor 488 goat anti-rabbit secondary antibody (1:500, Abcam, Cambridge, MA) for GFP. After three washes in PBS, the sections were mounted in Fluoromount-G (SouthernBiotech, Birmingham AL) or DAPI Fluoromount-G (SouthernBiotech). Images were captured using a confocal microscope (Olympus, Japan) at 20X or 100X objective, indicated by scale bars in images.

Statistical Analysis

For *in vitro* studies, a mixed-effects linear regression model treating CECs from different donors as a random effect was used to analyze the results. For *in vivo* studies, a mixed effects linear regression model with CNV lesions nested within the same eye was used to statistically analyze CNV volumes as previously described[14,35], and a two-sample t-test was used for protein analysis. Results are presented as mean±SEM. A P value < 0.05 was considered statistically significant. All statistical analyses were performed with STATA-14 software (StataCorp LLC, College Station, TX).

Results

Rap1 Activation Prevents CEC Migration and Tube Formation by Inhibiting VEGF-mediated Rac1 Activation.

We previously found that activation of Rap1 reduced CEC migration by TNFα-mediated Rac1 activation and NADPH oxidase generated ROS[12]. To test the prediction that increased Rap1GTP also antagonizes VEGF-induced Rac1 activation, we performed a dose-response experiment in which CECs were treated with different concentrations of 8CPT-AM, a Rap1 activator, in the presence of VEGF (50 ng/mL) or PBS. We found increased Rap1 activation with increasing concentrations of 8CPT-AM reduced VEGF-induced Rac1 activation in a dose-dependent manner (Fig. 1A–B). The data show activation of Rap1 interferes with VEGF-induced Rac1 activation.

We previously found sustained VEGF-induced Rac1 activation in CECs required Rac1GTP to be bound to the GRD of IQGAP1[14]. Since Rap1 interactions with IQGAP1 were reported to compete with binding of effectors to IQGAP1 domains using other cells[24], we predicted that increased Rap1GTP interactions with IQGAP1 would be associated with reduced VEGF-induced Rac1GTP. To test this, we treated cultured CECs with equal volumes of 8CPT-AM (1 μM) or 0.05% DMSO (control) in addition to VEGF or PBS. Compared to DMSO, 8CPT-AM increased Rap1 activation and Rap1GTP co-immunoprecipitated with IQGAP1 (Fig. 2A–B) and reduced VEGF-mediated Rac1GTP and Rac1GTP co-immunoprecipitated with IQGAP1 (Fig. 2C–D). In parallel experiments CEC migration (Fig. 2E–F) and tube formation (Fig. 2G–H) were similarly reduced in association with Rap1 activation by 8CPT-AM. Thus, our data suggest that increased Rap1GTP-IQGAP1 interactions are associated with reduced VEGF-induced Rac1 activation, CEC migration and tube formation.

Rap1GTP-binding to the IQ domain of IQGAP1 Interferes with Rac1 Activation.

In order to determine if Rap1GTP binding to the IQ domain of IQGAP1 in CECs reduced Rac1 activation and binding, we transfected CECs with GFP-tagged full length IQGAP1 (GFP-IQ-WT), which overexpressed IQGAP1, or GFP-tagged IQGAP1 with the IQ domain deleted (GFP-IQ-ΔIQ)[28]. In cultured CECs, the GFP-IQ-ΔIQ construct reduced Rap1GTP binding IQGAP1 compared to GFP-IQ-WT (Supplementary Fig. 1A), and the expressed GFP-IQ-WT and GFP-IQ-ΔIQ proteins localized to similar subcellular compartments as endogenous IQGAP1 (Supplementary Fig. 1C). Following treatment with 8CPT-AM or DMSO and either VEGF or PBS for 30 minutes, CECs transfected with the GFP-IQ-ΔIQ construct had significantly increased VEGF-induced Rac1GTP compared to CECs transfected with GFP-IQ-WT (Fig. 3A, Rows 1 and 2, Columns 2 vs. 6, and 4 vs. 8; Fig. 3B). 8CPT-AM did not increase Rap1GTP co-localization with GFP-tagged IQGAP1 in CECs transfected with GFP-IQ-ΔIQ compared to CECs transfected with GFP-IQ-WT (Fig. 3C–D). These data suggest that active Rap1 binding to the IQ domain of IQGAP1 is necessary to antagonize VEGF-induced Rac1 activation in CECs.

To determine whether Rap1 binding was sufficient to prevent Rac1 activation, we used a Myc-tagged IQGAP1 construct that contained point mutations in selected arginine residues to glutamine in the IQ domain (Myc-IQ-3,4R) and enhanced Rap1GTP binding[24] compared to the Myc-IQ-WT control (Supplementary Fig. 1B). Following treatment with VEGF or PBS and either 8CPT-AM or DMSO, CECs transfected with Myc-IQ-3,4R and treated with 8CPT-AM had significantly less VEGF-induced Rac1GTP compared to Myc-IQ-WT (Fig. 4A, Rows 1 and 2, Column 4 vs. 8; Fig. 4B). Given the effect of the Myc-IQ-3,4R mutant in increasing Rap1GTP binding, the data support the notion that Rap1GTP binding of IQGAP1 is sufficient to interfere with VEGF-mediated Rac1 activation in CECs. Together, the results from Figures 3 and 4 suggest Rap1GTP binding the IQ domain of IQGAP1 is both necessary and sufficient to prevent VEGF-mediated Rac1 activation in CECs.

Activation of Rap1a Prevents VEGF-mediated Rac1 Activation, Cell Migration, and Tube Formation.

Rap1 has two isoforms that are 95% homologous[37], Rap1a and Rap1b, and both isoforms bind to IQGAP1[24,38]. However, deficiency of Rap1a, but not Rap1b, led to VEGF-mediated permeability in endothelial cells[39]. Furthermore, we previously found that expression of active Rap1a was sufficient to reduce CEC activation and migration induced by TNFα[12]. Therefore, we tested the prediction that activation of Rap1a would sufficiently reduce VEGF-mediated CEC activation and migration. CECs were incubated with an adenovirus expressing either GFP (Ad-GFP) or GFP-tagged constitutively active Rap1a (Ad-GFP-63E)[12,15] (Fig. 5A–B) and treated with equal volumes of either PBS or VEGF for 30 minutes. VEGF-mediated Rac1GTP was prevented in CECs transduced with Ad-GFP-63E compared to Ad-GFP (Fig. 5C–D). In addition, VEGF-mediated CEC migration (Fig. 5E–F) and tube formation (Fig. 5G–H) were prevented in CECs transduced with Ad-GFP-63E compared to Ad-GFP. These data suggest that active Rap1a is also sufficient to prevent VEGF-mediated CEC migration and tube formation.

Endothelial IQGAP1 is Required for Active Rac1-Mediated Choroidal Neovascularization.

Since IQGAP1 binding Rac1GTP is necessary to sustain Rac1 activation in CECs[14], we postulated that endothelial-specific deletion of IQGAP1 would reduce CNV as a result of loss of Rac1GTP-IQGAP1 interactions. To test this hypothesis, we used the Cre-lox system to generate mice with an inducible deletion of IQGAP1 specifically in endothelial cells and determined their response to laser-induced CNV. We first validated our endothelium-specific knockout mouse model by administering tamoxifen to induce IQGAP1 deletion to four-week-old mice ($IQ^{i\Delta EC}$) and littermate control mice (IQ^{fl}) (Fig. 6A). Cre-mediated recombination of the floxed IQGAP1 allele was confirmed by PCR of DNA isolated from ear punches (Fig. 6B) and Cre-mediated recombination of the floxed YFP allele to permit expression of YFP in endothelial cells was confirmed through live fluorescence imaging of the retina using the Micron IV (Fig. 6C). To validate endothelial-specific activation of Cre recombinase in the choroid, we performed immunohistochemical staining of posterior eye cup cross-sections. IQGAP1 was present in lectin-stained vessels in IQ^{fl}, whereas IQGAP1 expression was not present in lectin-stained CECs of $IQ^{i\Delta EC}$ (Fig. 6D). We then performed laser to induce CNV and found significantly reduced CNV volumes in $IQ^{i\Delta EC}$ compared to littermate IQ^{fl} (Fig. 7A–B, Supplementary Fig. 2A). (Laser-induced CNV was lower in female compared to male control tamoxifen-treated IQ^{fl}, which lacked Cre, Supplementary Fig. 2B). We also observed significantly reduced Rac1GTP co-localization with lectin-stained CNV lesions compared to littermate IQ^{fl} (Fig. 7C–D). Since VEGF signaling through its angiogenic receptor, VEGFR2, has been implicated in murine laser-induced CNV development[40,41] and nAMD pathogenesis[42,43], we measured VEGF and VEGFR2 levels in RPE/choroids from $IQ^{i\Delta EC}$ and littermate IQ^{fl}. Normalized VEGF and VEGFR2 levels were not significantly changed between $IQ^{i\Delta EC}$ and their littermate IQ^{fl} controls (Supplementary Fig. 2C–D). Together, the data support the hypothesis that endothelial IQGAP1 mediates Rac1GTP-induced CNV independent of VEGF/VEGFR2 protein levels. These findings suggest that Rac1GTP-IQGAP1 interactions in endothelial cells are important in the development of CNV.

Rap1GTP Interactions with Endothelial IQGAP1 are Required to Protect Against Laser-Induced CNV.

We previously found a significant reduction in laser-induced CNV in C57Bl/6J mice treated with intravitreal 8CPT to increase broad Rap1 activation[26]. In addition, gene therapy to introduce constitutively active Rap1a through adeno-associated virus 2 specifically into RPE cells also reduced CNV after laser[44,45]. $IQ^{i\Delta EC}$ had reduced CNV volume due to reduced Rac1GTP expression and we determined if treatment with intravitreal 8CPT to broadly activate Rap1, including in the RPE, would further reduce CNV after laser compared to IQ^{fl} treated with 8CPT. However, we observed no difference in laser-induced CNV volumes between IQ^{fl} treated with intravitreal 8CPT and $IQ^{i\Delta EC}$ treated with intravitreal 8CPT (Fig. 8A–B). This finding suggests that a main effect of active Rap1 in CNV requires interactions with IQGAP1 in endothelial cells.

Discussion

nAMD is one of the leading causes of blindness worldwide[46]. Vision loss is associated with activated CECs that transmigrate the RPE monolayer to form vision-threatening CNV in the neural retina. The standard of care is use of agents that interfere with the bioactivity of VEGF[47]; however, anti-VEGF agents have improved visual acuity in only 40% of patients[6,48,49]. Reasons may involve multiple age-related stresses that crosstalk to activate downstream effectors of VEGF signaling to promote pathology. Our previous studies identified Rac1GTP as a common downstream effector of inflammatory (e.g., TNFα)[12], angiogenic (e.g., VEGF and CCL11)[14,50], and oxidative (e.g., NADPH oxidase-generated ROS) signaling pathways, which are implicated in nAMD pathology. We previously found Rac1GTP was required for CEC transmigration of the RPE and was involved in laser-induced CNV[14,20]. Furthermore, we observed that Rac1GTP was sustained when bound to the GRD of IQGAP1 in CECs[14]. These results suggest binding between Rac1GTP and IQGAP1 is necessary to activate CECs and promote cell migration into the neural retina as vision-threatening CNV. Since Rac1 inhibitors are inefficient[51,52], and Rac1 has physiologic effects[21], we seek methods to regulate Rac1 activation as a means to reduce CNV. Broad activation of Rap1GTP or increased activation of Rap1aGTP in the RPE reduced laser-induced CNV. In other cells, Rap1GTP can bind the IQ domain of IQGAP1 and interfere with other GTPases binding the GRD[24]. This prompted us to test the hypothesis that Rap1GTP binding the IQ domain of IQGAP1 in CECs prevents CNV by interfering with Rac1 activation.

Using cultured CECs from human donors with low to moderate AMD risk profile, we found that 8CPT reduced VEGF-mediated Rac1 activation, CEC migration and tube formation but increased Rap1GTP interactions with IQGAP1. These findings extend our previous findings in which the inflammatory cytokine, TNFα, activated Rac1, whereas pharmacologic activation of Rap1 with 8CPT reduced TNFα-induced Rac1 activation[12]. However, other studies have reported that VEGF increases Rap activation[53]. We did not observe VEGF-induced Rap1 activation in cultured CECs (Figs. 1 and 2), but we cannot rule out the possibility that VEGF increased other Rap family members, such as Rap2[54], which we did not measure. Previous studies have also reported increased cell proliferation to 8CPT in

other types of cultured endothelial cells[55]. Based on the data, there may be a difference in VEGF-induced Rap1 activation among different cell types. Our data, however, suggest that an interaction of Rap1 with IQGAP1 in CECs interfered with Rac1 activation.

We also observed 8CPT-induced Rap1GTP binding the IQ domain was both necessary and sufficient to reduce Rac1 activation. We, however, found a modest increase in VEGF-induced Rac1 activation in CECs transfected with wild type IQGAP1 (GFP-IQ-WT and Myc-IQ-WT) (Figs. 3 and 4). We found significant VEGF-induced Rac1 activation in non-transfected CECs (Fig. 2) and we previously found knockdown of IQGAP1 by siRNA abolished VEGF-induced Rac1 in CECs[14]. CECs transfected with GFP-IQ-WT and Myc-IQ-WT overexpress IQGAP1. Overexpression of IQGAP1 increases the activation of small GTPases (i.e., Cdc42 and Rac1) in unstimulated cells[56–58]. We speculate overexpression may lead to greater basal IQGAP1-Rac1GTP binding, thereby reducing the increase expected with VEGF treatment. Myc-IQ-3,4R transfected CECs had reduced Rac1GTP compared to Myc-IQ-WT transfected CECs, but some Rap1GTP even in the absence of 8CPT (Fig. 4). We speculate CECs transfected with Myc-IQ-3,4R have basal Rap1GTP binding to IQGAP1 that reduces Rac1GTP in both control and VEGF-treated CECs. Our findings still support the notion that Rap1GTP binding to IQGAP1 reduces Rac1 activation.

We previously observed *Iqgap1*$^{-/-}$ mice had significantly reduced laser-induced CNV and Rac1GTP co-localization with lectin-stained CNV lesions in cryo-sections compared to littermate *Iqgap1*$^{+/+}$ mice[14]. Since IQGAP1 interacts with both Rac1GTP and Rap1GTP, we determined if endothelial IQGAP1 would be necessary for laser-induced CNV through the binding of active Rac1 to the GRD. Tamoxifen-inducible endothelial IQGAP1 knockout mice (IQ$^{i\Delta EC}$) in the murine laser-induced CNV model had significantly reduced CNV volumes and Rac1GTP co-localization with lectin-stained CNV lesions compared to tamoxifen-injected littermate control mice (IQ^{fl}) (Fig. 7). Our findings in IQ$^{i\Delta EC}$ corroborated our results from *Iqgap1*$^{-/-}$ mice. We, however, also found that tamoxifen-injected female IQ^{fl}, compared to male IQ^{fl}, had significantly reduced CNV. Previous studies reported tamoxifen to have an anti-angiogenic effect by inhibiting the secretion of VEGF from epithelial cells[59]. However, neither male nor female IQ$^{i\Delta EC}$ and IQ^{fl} had differences in VEGF or VEGFR2 levels in RPE/choroids. We also did not observe sex differences in CNV volumes in *Iqgap1*$^{-/-}$ mice compared to *Iqgap1*$^{+/+}$ mice, suggesting that sex effects were due to tamoxifen-mediated inhibition of laser-induced CNV and warrant future studies. Nonetheless, these findings support the hypothesis that endothelial IQGAP1 regulates Rac1-induced CNV independent from VEGF and VEGFR2 concentrations.

Rap1 activation reduced CEC activation and migration by interacting with IQGAP1 *in vitro*. Similarly, *in vivo*, we found pharmacologic activation of Rap1 with 8CPT significantly reduced CNV in IQ^{fl} mice and did not further reduce CNV in IQ$^{i\Delta EC}$ (Fig. 8). These findings point to the importance of Rap1GTP interactions with IQGAP1 in endothelial cells to interfere with CNV. There was a reduced fold effect from 8CPT in control IQ^{fl} treated with tamoxifen compared to our earlier studies[15,26] potentially related to tamoxifen effects in female mice that reduced baseline laser-induced CNV volumes and masked the effect from intravitreal 8CPT. Still, this did not diminish the importance of endothelial Rap1-IQGAP1 interactions in reducing CNV.

In conclusion, our study supports the hypothesis that Rap1GTP binding to the IQ domain of IQGAP1 can prevent Rac1 activation in CECs, which is an important molecular event that leads to CNV (Fig. 9). The findings from our study also support the hypothesis that interactions between IQGAP1 and Rap1GTP are sufficient to reduce Rac1 activation in CECs and prevent the development of vision-threatening CNV.

Supplementary Material

Refer to Web version on PubMed Central for supplementary material.

Acknowledgements

This study was supported by the National Institutes of Health EY014800 and an Unrestricted Grant from Research to Prevent Blindness, Inc., New York, NY, to the Department of Ophthalmology & Visual Sciences, University of Utah; and the National Institutes of Health R01EY015130 and R01EY017011 to MEH. BC is supported by R01EY024998. DBS is supported by the Intramural Research Program of the National Institutes of Health.

Nonstandard abbreviations:

CNV	choroidal neovascularization
nAMD	neovascular age-related macular degeneration
CECs	choroidal endothelial cells

References

1. Wong WL, Su X, Li X, et al. Global prevalence of age-related macular degeneration and disease burden projection for 2020 and 2040: a systematic review and meta-analysis. Lancet Glob Health. 2014;2(2):e106–116. [PubMed: 25104651]
2. Stevens TS, Bressler NM, Maguire MG, et al. Occult choroidal neovascularization in age-related macular degeneration. A natural history study. Archives of Ophthalmology. 1997;115:345–350. [PubMed: 9076206]
3. Hartnett ME, Elsner AE. Characteristics of exudative age-related macular degeneration determined in vivo with confocal and indirect infrared imaging. Ophthalmology. 1996;103:58–71. [PubMed: 8628562]
4. Joussen AM, Bornfeld N. The treatment of wet age-related macular degeneration. Dtsch Arztebl Int. 2009;106(18):312–317. [PubMed: 19547647]
5. Haller JA. Current anti-vascular endothelial growth factor dosing regimens: benefits and burden. Ophthalmology. 2013;120(5 Suppl):S3–7. [PubMed: 23642784]
6. Rofagha S, Bhisitkul RB, Boyer DS, Sadda SR, Zhang K. Seven-Year Outcomes in Ranibizumab-Treated Patients in ANCHOR, MARINA, and HORIZON: A Multicenter Cohort Study (SEVEN-UP). Ophthalmology. 2013.
7. Keenan TD, Toso M, Pappas C, Nichols L, Bishop PN, Hageman GS. Assessment of Proteins Associated With Complement Activation and Inflammation in Maculae of Human Donors Homozygous Risk at Chromosome 1 CFH-to-F13B. Investigative ophthalmology & visual science. 2015;56(8):4870–4879. [PubMed: 26218915]
8. Cao S, Wang JCC, Gao J, et al. CFH Y402H polymorphism and the complement activation product C5a: effects on NF-κB activation and inflammasome gene regulation. British Journal of Ophthalmology. 2016.
9. Toomey CB, Kelly U, Saban DR, Bowes Rickman C. Regulation of age-related macular degeneration-like pathology by complement factor H. Proceedings of the National Academy of Sciences of the United States of America. 2015;112(23):E3040–3049. [PubMed: 25991857]

10. Seddon JM, Silver RE, Kwong M, Rosner B. Risk Prediction for Progression of Macular Degeneration: 10 Common and Rare Genetic Variants, Demographic, Environmental, and Macular Covariates. Investigative ophthalmology & visual science. 2015;56(4):2192–2202. [PubMed: 25655794]
11. Gragoudas ES, Adamis AP, Cunningham ET Jr., Feinsod M, Guyer DR, Group. tVISiONCT. Pegaptanib for neovascular age-related macular degeneration. The New England journal of medicine. 2004;351(27):2805–2816. [PubMed: 15625332]
12. Wang H, Fotheringham L, Wittchen ES, Hartnett ME. Rap1 GTPase Inhibits Tumor Necrosis Factor-alpha-Induced Choroidal Endothelial Migration via NADPH Oxidase- and NF-kappaB-Dependent Activation of Rac1. Am J Pathol. 2015;185(12):3316–3325. [PubMed: 26476350]
13. Monaghan-Benson E, Hartmann J, Vendrov AE, et al. The Role of Vascular Endothelial Growth Factor-Induced Activation of NADPH Oxidase in Choroidal Endothelial Cells and Choroidal Neovascularization. The American Journal of Pathology. 2010;177(4):2091–2102. [PubMed: 20802176]
14. Wang H, Ramshekar A, Kunz E, Sacks DB, Hartnett ME. IQGAP1 causes choroidal neovascularization by sustaining VEGFR2-mediated Rac1 activation. Angiogenesis. 2020.
15. Wang H, Jiang Y, Shi D, et al. Activation of Rap1 inhibits NADPH oxidase-dependent ROS generation in retinal pigment epithelium and reduces choroidal neovascularization. FASEB journal : official publication of the Federation of American Societies for Experimental Biology. 2014;28(1):265–274. [PubMed: 24043260]
16. Burridge K, Wennerberg K. Rho and Rac take center stage. Cell. 2004;116(2):167–179. [PubMed: 14744429]
17. Fukata M, Nakagawa M, Kaibuchi K. Roles of Rho-family GTPases in cell polarisation and directional migration. Current Opinion In Cell Biology. 2003;15(5):590–597. [PubMed: 14519394]
18. Ridley AJ, Schwartz MA, Burridge K, et al. Cell migration: integrating signals from front to back. Science (New York, NY). 2003;302(5651):1704–1709.
19. Soga N, Namba N, McAllister S, et al. Rho family GTPases regulate VEGF-stimulated endothelial cell motility. Experimental cell research. 2001;269(1):73–87. [PubMed: 11525641]
20. Peterson LJ, Wittchen ES, Geisen P, Burridge K, Hartnett ME. Heterotypic RPE-choroidal endothelial cell contact increases choroidal endothelial cell transmigration via PI 3-kinase and Rac1. Experimental Eye Research. 2007;84(4):737–744. [PubMed: 17292356]
21. Panday A, Sahoo MK, Osorio D, Batra S. NADPH oxidases: an overview from structure to innate immunity-associated pathologies. Cell Mol Immunol. 2015;12(1):5–23. [PubMed: 25263488]
22. Hedman AC, Smith JM, Sacks DB. The biology of IQGAP proteins: beyond the cytoskeleton. EMBO Rep. 2015;16(4):427–446. [PubMed: 25722290]
23. Malarkannan S, Awasthi A, Rajasekaran K, et al. IQGAP1: a regulator of intracellular spacetime relativity. J Immunol. 2012;188(5):2057–2063. [PubMed: 22345702]
24. Jeong HW, Li Z, Brown MD, Sacks DB. IQGAP1 binds Rap1 and modulates its activity. The Journal of biological chemistry. 2007;282(28):20752–20762. [PubMed: 17517894]
25. Li J, Zhang R, Wang C, et al. Activation of the Small GTPase Rap1 Inhibits Choroidal Neovascularization by Regulating Cell Junctions and ROS Generation in Rats. Current eye research. 2018;43(7):934–940. [PubMed: 29601231]
26. Wittchen ES, Nishimura E, McCloskey M, et al. Rap1 GTPase Activation and Barrier Enhancement in RPE Inhibits Choroidal Neovascularization In Vivo. PloS one. 2013;8(9):e73070. [PubMed: 24039860]
27. Zouache MA, Bennion A, Hageman JL, Pappas C, Richards BT, Hageman GS. Macular retinal thickness differs markedly in age-related macular degeneration driven by risk polymorphisms on chromosomes 1 and 10. Scientific reports. 2020;10(1):21093. [PubMed: 33273512]
28. Sokol SY, Li Z, Sacks DB. The effect of IQGAP1 on Xenopus embryonic ectoderm requires Cdc42. The Journal of biological chemistry. 2001;276(51):48425–48430. [PubMed: 11584017]
29. Li Z, Sacks DB. Elucidation of the interaction of calmodulin with the IQ motifs of IQGAP1. The Journal of biological chemistry. 2003;278(6):4347–4352. [PubMed: 12446675]

30. Nowak-Sliwinska P, Alitalo K, Allen E, et al. Consensus guidelines for the use and interpretation of angiogenesis assays. Angiogenesis. 2018;21(3):425–532. [PubMed: 29766399]
31. Farley FW, Soriano P, Steffen LS, Dymecki SM. Widespread recombinase expression using FLPeR (flipper) mice. Genesis. 2000;28(3–4):106–110. [PubMed: 11105051]
32. Srinivas S, Watanabe T, Lin CS, et al. Cre reporter strains produced by targeted insertion of EYFP and ECFP into the ROSA26 locus. BMC Dev Biol. 2001;1:4. [PubMed: 11299042]
33. Lee S, Elaskandrany M, Lau LF, Lazzaro D, Grant MB, Chaqour B. Interplay between CCN1 and Wnt5a in endothelial cells and pericytes determines the angiogenic outcome in a model of ischemic retinopathy. Scientific reports. 2017;7(1):1405. [PubMed: 28469167]
34. Sorensen I, Adams RH, Gossler A. DLL1-mediated Notch activation regulates endothelial identity in mouse fetal arteries. Blood. 2009;113(22):5680–5688. [PubMed: 19144989]
35. Bretz CA, Divoky V, Prchal J, et al. Erythropoietin Signaling Increases Choroidal Macrophages and Cytokine Expression, and Exacerbates Choroidal Neovascularization. Scientific reports. 2018;8(1):2161. [PubMed: 29391474]
36. Lambert V, Lecomte J, Hansen S, et al. Laser-induced choroidal neovascularization model to study age-related macular degeneration in mice. Nat Protoc. 2013;8(11):2197–2211. [PubMed: 24136346]
37. Wittchen ES, Aghajanian A, Burridge K. Isoform-specific differences between Rap1A and Rap1B GTPases in the formation of endothelial cell junctions. Small GTPases. 2011;2(2):65–76. [PubMed: 21776404]
38. Awasthi A, Samarakoon A, Chu H, et al. Rap1b facilitates NK cell functions via IQGAP1-mediated signalosomes. The Journal of experimental medicine. 2010;207(9):1923–1938. [PubMed: 20733035]
39. Lakshmikanthan S, Sobczak M, Li Calzi S, Shaw L, Grant MB, Chrzanowska-Wodnicka M. Rap1B promotes VEGF-induced endothelial permeability and is required for dynamic regulation of the endothelial barrier. J Cell Sci. 2018;131(1).
40. Gu L, Chen H, Tuo J, Gao X, Chen L. Inhibition of experimental choroidal neovascularization in mice by anti-VEGFA/VEGFR2 or non-specific siRNA. Exp Eye Res. 2010;91(3):433–439. [PubMed: 20599960]
41. Huang H, Parlier R, Shen JK, Lutty GA, Vinores SA. VEGF receptor blockade markedly reduces retinal microglia/macrophage infiltration into laser-induced CNV. PloS one. 2013;8(8):e71808. [PubMed: 23977149]
42. Huang H, Shen J, Vinores SA. Blockade of VEGFR1 and 2 suppresses pathological angiogenesis and vascular leakage in the eye. PloS one. 2011;6(6):e21411. [PubMed: 21731737]
43. Cruz-Gonzalez F, Cabrillo-Estevez L, Lopez-Valverde G, Cieza-Borrella C, Hernandez-Galilea E, Gonzalez-Sarmiento R. Predictive value of VEGF A and VEGFR2 polymorphisms in the response to intravitreal ranibizumab treatment for wet AMD. Graefe's archive for clinical and experimental ophthalmology = Albrecht von Graefes Archiv fur klinische und experimentelle Ophthalmologie. 2014;252(3):469–475.
44. Wang H, Han X, Bretz CA, et al. Retinal pigment epithelial cell expression of active Rap 1a by scAAV2 inhibits choroidal neovascularization. Molecular therapy Methods & clinical development. 2016;3:16056. [PubMed: 27606349]
45. Wang H, Kunz E, Stoddard GJ, Hauswirth WW, Hartnett ME. Optimal Inhibition of Choroidal Neovascularization by scAAV2 with VMD2 Promoter-driven Active Rap1a in the RPE. Scientific reports. 2019;9(1):15732. [PubMed: 31673119]
46. Prokofyeva E, Zrenner E. Epidemiology of major eye diseases leading to blindness in Europe: a literature review. Ophthalmic Res. 2012;47(4):171–188. [PubMed: 22123077]
47. Solomon SD, Lindsley K, Vedula SS, Krzystolik MG, Hawkins BS. Anti-vascular endothelial growth factor for neovascular age-related macular degeneration. The Cochrane database of systematic reviews. 2019;3:CD005139. [PubMed: 30834517]
48. Gillies MC, Campain A, Barthelmes D, et al. Long-Term Outcomes of Treatment of Neovascular Age-Related Macular Degeneration: Data from an Observational Study. Ophthalmology. 2015;122(9):1837–1845. [PubMed: 26096346]

49. Otsuji T, Nagai Y, Sho K, et al. Initial non-responders to ranibizumab in the treatment of age-related macular degeneration (AMD). Clin Ophthalmol. 2013;7:1487–1490. [PubMed: 23901256]
50. Wang H, Han X, Gambhir D, et al. Retinal Inhibition of CCR3 Induces Retinal Cell Death in a Murine Model of Choroidal Neovascularization. PloS one. 2016;11(6):e0157748. [PubMed: 27309355]
51. Bid HK, Roberts RD, Manchanda PK, Houghton PJ. RAC1: an emerging therapeutic option for targeting cancer angiogenesis and metastasis. Mol Cancer Ther. 2013;12(10):1925–1934. [PubMed: 24072884]
52. Bergers G, Benjamin LE. Tumorigenesis and the angiogenic switch. Nat Rev Cancer. 2003;3(6):401–410. [PubMed: 12778130]
53. Chrzanowska-Wodnicka M, Kraus AE, Gale D, White GC 2nd, Vansluys J Defective angiogenesis, endothelial migration, proliferation, and MAPK signaling in Rap1b-deficient mice. Blood. 2008;111(5):2647–2656. [PubMed: 17993608]
54. Goitre L, Trapani E, Trabalzini L, Retta SF. The Ras superfamily of small GTPases: the unlocked secrets. Methods Mol Biol. 2014;1120:1–18. [PubMed: 24470015]
55. Namkoong S, Kim CK, Cho YL, et al. Forskolin increases angiogenesis through the coordinated crosstalk of PKA-dependent VEGF expression and Epac-mediated PI3K/Akt/eNOS signaling. Cellular signalling. 2009;21(6):906–915. [PubMed: 19385062]
56. Noritake J, Fukata M, Sato K, et al. Positive role of IQGAP1, an effector of Rac1, in actin-meshwork formation at sites of cell-cell contact. Mol Biol Cell. 2004;15(3):1065–1076. [PubMed: 14699063]
57. Swart-Mataraza JM, Li Z, Sacks DB. IQGAP1 is a component of Cdc42 signaling to the cytoskeleton. The Journal of biological chemistry. 2002;277(27):24753–24763. [PubMed: 11948177]
58. Jadeski L, Mataraza JM, Jeong HW, Li Z, Sacks DB. IQGAP1 stimulates proliferation and enhances tumorigenesis of human breast epithelial cells. The Journal of biological chemistry. 2008;283(2):1008–1017. [PubMed: 17981797]
59. Garvin S, Dabrosin C. Tamoxifen inhibits secretion of vascular endothelial growth factor in breast cancer in vivo. Cancer Res. 2003;63(24):8742–8748. [PubMed: 14695189]

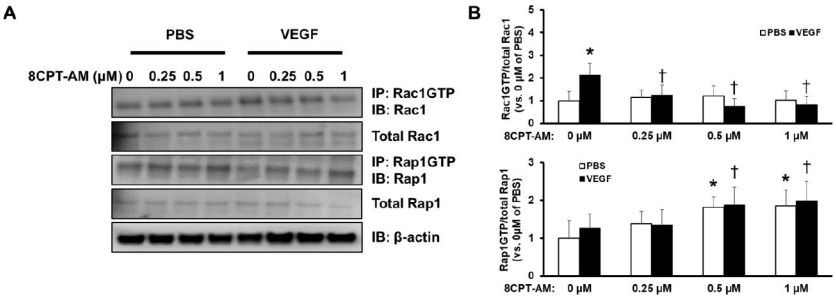

Fig. 1. Rap1 activation reduces VEGF-induced Rac1 activation in a dose-dependent manner.

A) Representative western blot images depicting Rac1 activation by immunoprecipitation of Rac1GTP and blot of total Rac1 (row 1), total Rac1 (row 2), Rap1 activation by immunoprecipitation of Rap1GTP and blot of total Rap1 (row 3), total Rap1 (row 4), and β-actin (row 5) in lysates from CECs treated with 0.05% DMSO (0 μM 8CPT-AM), 0.25 μM, 0.5 μM, or 1 μM of 8CPT-AM in the presence of PBS or VEGF (50 ng/mL). B) Quantification of Rac1 activation (top) and Rap1 activation (bottom) by densitometry analysis (Normalized mean±SEM, *$p<0.05$ vs. 0 μM of PBS, $^{\dagger}p<0.05$ vs. 0 μM of VEGF, n=3 per group from 3 independent experiments)

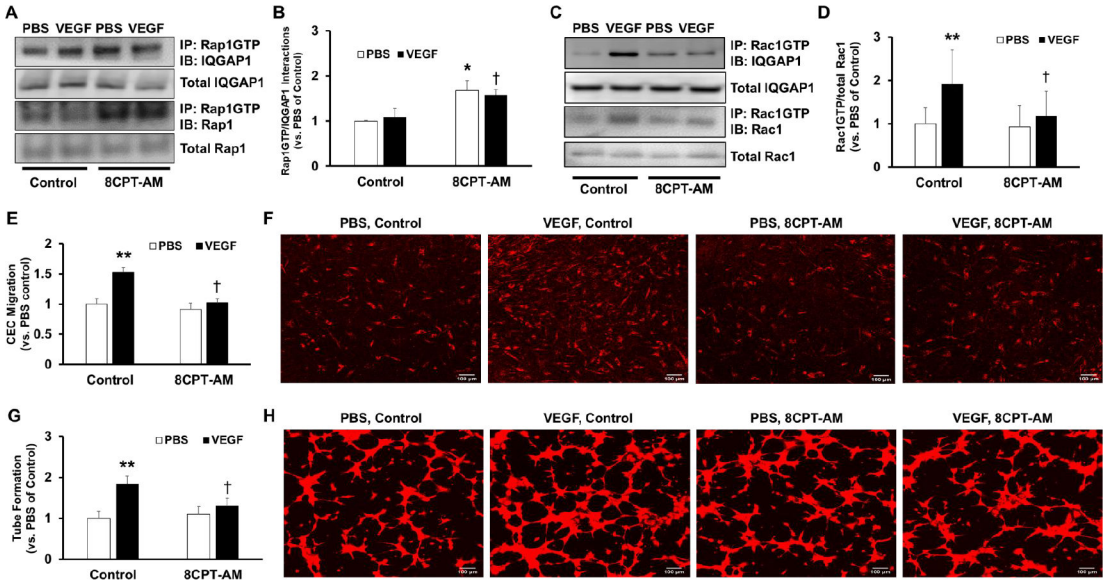

Fig. 2. Rap1 activation reduces VEGF-induced Rac1 activation, migration, and tube formation by interacting with IQGAP1 in CECs.

A) Representative western blot images that show Rap1GTP interactions with IQGAP1 determined by co-immunoprecipitation (row 1), total IQGAP1 (row 2), Rap1 activation by immunoprecipitation (row 3), and total Rap1 (row 4) in lysates from CECs treated with PBS and 0.05% DMSO (Control), VEGF (50 ng/mL) and Control, PBS and 8CPT-AM (1 μM), or VEGF and 8CPT-AM for 30 minutes; B) Quantification of Rap1GTP interactions with IQGAP1 by densitometry analysis (Normalized mean±SEM, *p<0.05 vs. PBS of Control, †p<0.05 vs. VEGF of Control, n=3 per group from 3 independent experiments); C) Representative western blot images depicting Rac1GTP interactions with IQGAP1 determined by co-immunoprecipitation (row 1), total IQGAP1 (row 2), Rac1 activation by immunoprecipitation of Rac1GTP and blot of total Rac1 (row 3), and total Rac1 (row 4) in lysates from CECs treated similarly as Fig. 2A; D) Quantification of Rac1 activation by densitometry analysis (Normalized mean±SEM, **p<0.05 vs. PBS of Control, †p<0.05 vs. VEGF of Control, n=3 per group from 3 independent experiments); E) Quantification of migrated CECs on underside of Transwell insert in response to overnight treatment with 0.05% DMSO (Control) or 8CPT-AM (1 μM) in the presence of VEGF (50 ng/mL) or PBS (Normalized mean±SEM, **p<0.05 vs. PBS of Control, †p<0.05 vs. VEGF of Control, n=9 per group from 3 independent experiments); F) Representative confocal images of Vybrant-stained CECs on the underside of Transwell inserts in response to treatments described in Fig. 2E; G) Quantification of tube formation in CECs treated with 0.05% DMSO (Control) or 8CPT-AM (1 μM) in the presence of VEGF (50 ng/mL) or PBS for 12 hours (Normalized mean±SEM, **p<0.05 vs. PBS of Control, †p<0.05 vs. VEGF of Control, n=9 per group from 3 independent experiments); H) Representative fluorescent images of tube formation using Vybrant-stained CECs grown on top of Matrigel in response to treatments described in Fig. 2G

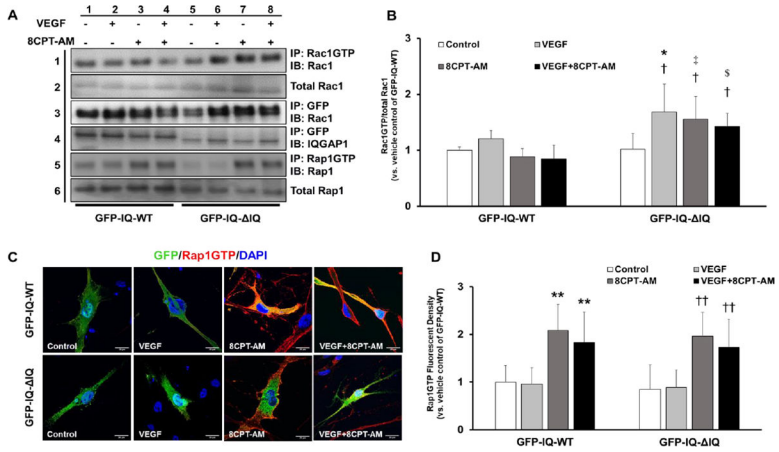

Fig. 3. Active Rap1 binding the IQ domain of IQGAP1 is necessary to reduce VEGF-induced Rac1 activation in CECs.

A) Representative western blot images that depict Rac1 activation by immunoprecipitation of Rac1GTP and blot of total Rac1 (row 1), total Rac1 (row 2), GFP-tagged IQGAP1 plasmid construct (i.e., either GFP-IQ-WT or GFP-IQ-ΔIQ) interactions with Rac1 by co-immunoprecipitation (row 3), GFP-tagged IQGAP1 pulled down by immunoprecipitation as loading control (row 4), Rap1 activation by immunoprecipitation (row 5), and total Rap1 (row 6) in lysates from CECs transfected with GFP-IQ-WT (columns 1–4) or GFP-IQ-ΔIQ (columns 5–8) and treated with 0.05% DMSO or 8CPT-AM (1 μM) in the presence VEGF (50 ng/mL) or PBS; B) Quantification of Rac1 activation by densitometry analysis (Normalized mean±SEM, $^{\dagger}p<0.05$ vs. Control of GFP-IQ-ΔIQ, *$p<0.05$ vs. VEGF of GFP-IQ-WT, $^{\ddagger}p<0.05$ vs. 8CPT-AM of GFP-IQ-WT, $^{\$}p<0.05$ vs. VEGF+8CPT-AM of GFP-IQ-WT, n=3 per group from 3 independent experiments); C) Representative confocal images of CECs labelled to identify GFP tagged IQGAP1 (green), Rap1GTP (red), and DAPI (blue) in response to 1 μL PBS and 0.05% DMSO (control), 50 ng/mL VEGF and 0.05% DMSO (VEGF), 1 μL PBS and 1 μM 8CPT-AM (8CPT-AM), or 50 ng/mL VEGF and 1 μM 8CPT-AM (VEGF+8CPT-AM); D) Quantification of Rap1GTP fluorescent density in response to treatments described in Fig. 3C (Normalized mean±SEM, **$p<0.05$ vs. Control of GFP-IQ-WT, $^{\dagger\dagger}p<0.05$ vs. Control of GFP-IQ-ΔIQ, n=3 per group from 3 independent experiments)

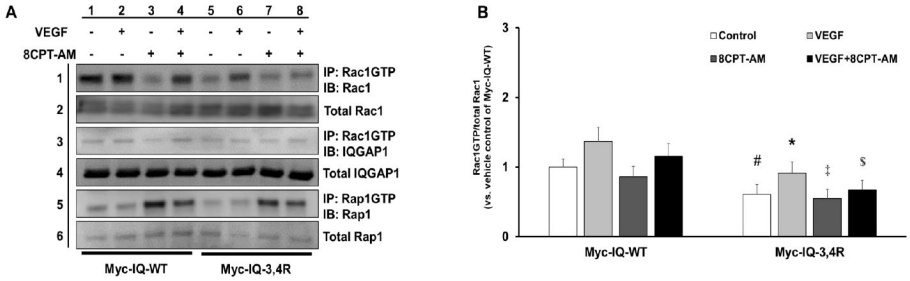

Fig. 4. Active Rap1 binding the IQ domain of IQGAP1 is sufficient to reduce VEGF-induced Rac1 activation in CECs.

A) Representative western blot images that depict Rac1 activation by immunoprecipitation of Rac1GTP and blot of total Rac1 (row 1), total Rac1 (row 2), Rac1GTP interactions with IQGAP1 by co-immunoprecipitation (row 3), total IQGAP1 (row 4), Rap1 activation to total Rap1 by co-immunoprecipitation (row 5), and total Rap1 (row 6) in lysates from CECs transfected with Myc-IQ-WT (columns 1–4) or Myc-IQ-3,4R (columns 5–8) and treated with 0.05% DMSO or 8CPT-AM (1 μM) in the presence VEGF (50 ng/mL) or PBS; B) Quantification of Rac1 activation by densitometry analysis (Normalized mean±SEM, $^{\#}p<0.05$ vs. Control of Myc-IQ-WT, $^{*}p<0.05$ vs. VEGF of Myc-IQ-WT, $^{‡}p<0.05$ vs. 8CPT-AM of Myc-IQ-WT, $^{\$}p<0.05$ vs. VEGF+8CPT-AM of Myc-IQ-WT, n=3 per group from 3 independent experiments)

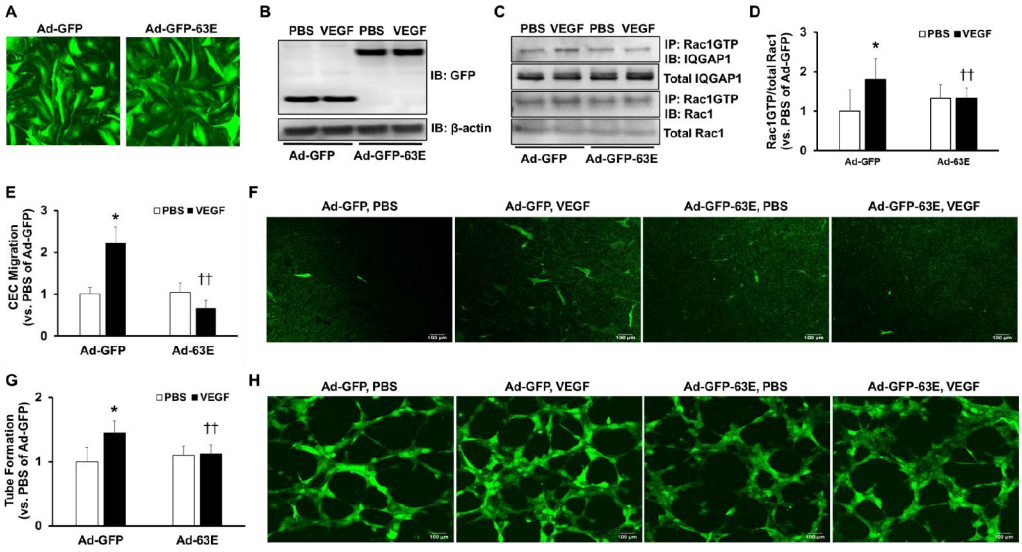

Fig. 5. Activation of Rap1a is sufficient to prevent VEGF-induced Rac1 activation, migration, and tube formation in CECs.

A) Representative images of CECs transduced with adenovirus expressing GFP (Ad-GFP) or constitutively active Rap1a (Ad-GFP-63E) 48 hours post-infection; B) Representative western blot images that depict expression of GFP (columns 1 and 2) or constitutively active Rap1a (columns 3 and 4) following 48 hours of transduction and treatment with equal volumes of PBS or VEGF (50 ng/mL) for 30 minutes; C) Representative western blot images that depict Rac1GTP interactions with IQGAP1 by co-immunoprecipitation (row 1), total IQGAP1 (row 2), Rac1 activation by immunoprecipitation of Rac1GTP and blot of total Rac1 (row 3), and total Rac1 (row 4) in lysates from CECs transduced with Ad-GFP (columns 1 and 2) or Ad-GFP-63E (columns 3 and 4) and treated with PBS (columns 1 and 3) or VEGF (50 ng/mL, columns 2 and 4) for 30 minutes; D) Quantification of Rac1 activation by densitometry analysis (Normalized mean±SEM, *$p<0.05$ vs. PBS of Ad-GFP, $^{\dagger\dagger}p<0.01$ vs. VEGF of Ad-GFP, n=3 per group from 3 independent experiments); E) Quantification of transduced CECs migrating in response to overnight treatment with VEGF (50 ng/mL) or PBS (Normalized mean±SEM, *$p<0.01$ vs. PBS of Ad-GFP, $^{\dagger\dagger}p<0.01$ vs. VEGF of Ad-GFP, n=9 per group from 3 independent experiments); F) Representative confocal images of transduced CECs on the underside of Transwell insert in response to treatments described in Fig. 5E; G) Quantification of tube formation in transduced CECs treated with PBS or VEGF (50 ng/mL) for 12 hours (Normalized mean±SEM, *$p<0.05$ vs. PBS of Ad-GFP, $^{\dagger\dagger}p<0.01$ vs. VEGF of Ad-GFP, n=9 per group from 3 independent experiments); H) Representative confocal images of tube formation using transduced CECs in response to conditions described in Fig. 5G

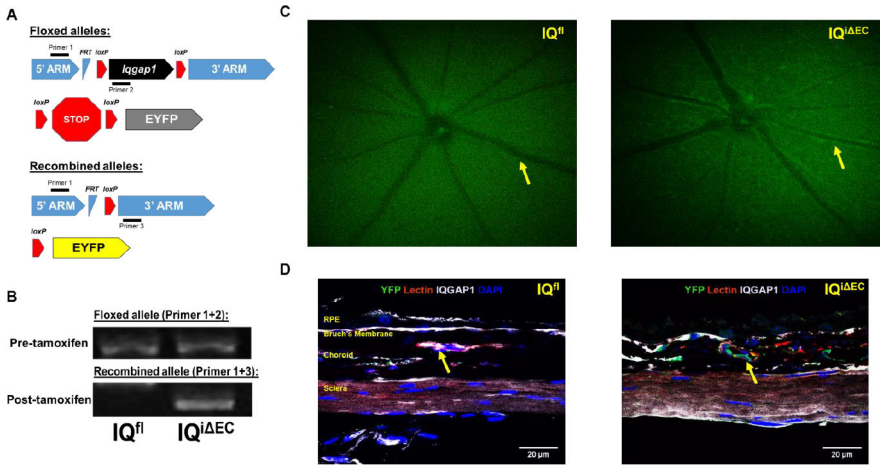

Fig. 6. Characterization of tamoxifen-inducible endothelial IQGAP1 knockout mouse model.

A) Diagram of floxed (top) and recombined (bottom) *Iqgap1* alleles that depict the locations of the designed primers for genotyping; B) PCR product demonstrating recombination of the floxed *Iqgap1* allele in tamoxifen-injected $IQ^{i\Delta EC}$ (bottom row, 2nd lane) and not in tamoxifen-injected IQ^{fl} mice (bottom row, 1st lane) using isolated DNA from ear punches; C) Representative images of live fluorescence imaging of the retina using the Micron IV that depict expression of YFP in endothelial cells in in tamoxifen-injected $IQ^{i\Delta EC}$ (right, yellow arrow) and not in tamoxifen-injected IQ^{fl} mice (left, yellow arrow); D) Representative confocal images of RPE/choroid/scleral tissues that demonstrate Cre-mediated recombination in tamoxifen-injected $IQ^{i\Delta EC}$ (right image) that were heterozygous for *Cdh5*-CreERT2 allele compared to no recombination in IQ^{fl} that lack *Cdh5*-CreERT2 (left image).Tamoxifen-injected $IQ^{i\Delta EC}$ show loss of IQGAP1 (white) co-localization with lectin-stained vessels (red) and expression of YFP in the choroid (right image), whereas tamoxifen-injected IQ^{fl} demonstrated IQGAP1 (white) co-localization with lectin-stained vessels (red) without YFP expression (left image)

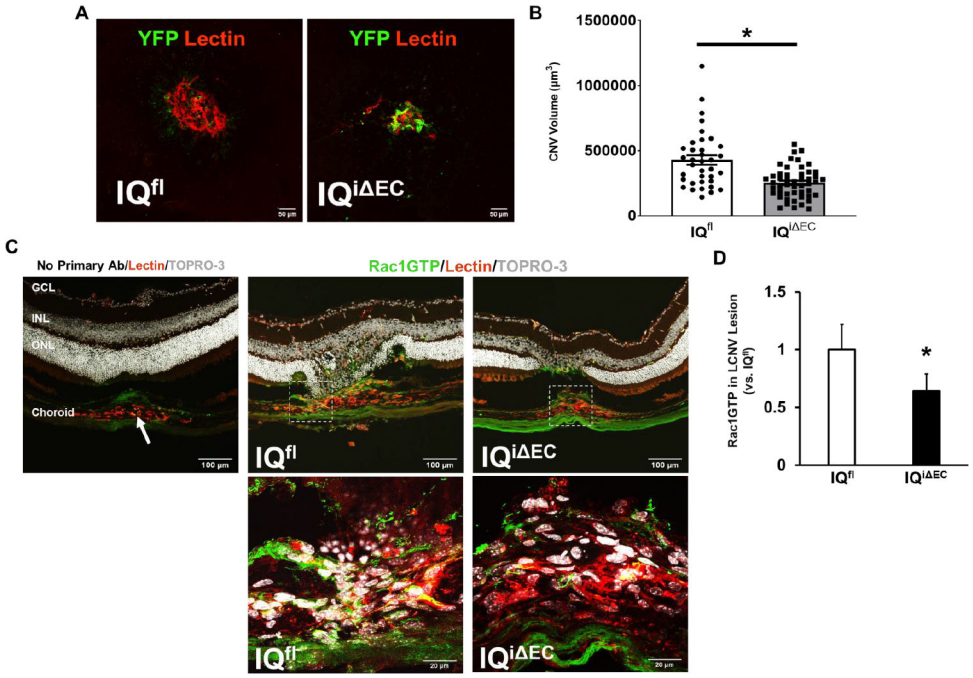

Fig. 7. Endothelial IQGAP1 is necessary for Rac1GTP-mediated CNV in the murine laser-induced CNV model.

A) Representative images of lectin-stained RPE/choroid flat mounts from IQ^{fl} showing no YFP and littermate $IQ^{i\Delta EC}$ showing YFP; B) Quantification of laser-induced CNV volume (Mean±SEM, *p<0.05 vs. IQ^{fl}, n=36 CNV lesions from 9 different mice for IQ^{fl} and n=49 CNV lesions from 13 different mice; C) Representative confocal images of posterior eye cup sections that were co-labeled with antibodies against Rac1GTP (green), lectin (red), and TOPRO-3 (grey) in IQ^{fl} (middle column) and $IQ^{i\Delta EC}$ (right column) at either 20X (top row) or 100X (bottom row) objective, staining with secondary antibody along with lectin and TOPRO-3 (left) was also performed in the absence of primary Rac1GTP antibody to determine non-specific fluorescence from secondary antibody in CNV lesion (white arrow); D) Quantification of Rac1GTP fluorescent density in lectin-labeled CNV lesion (Normalized mean±SEM, *p<0.05 vs. IQ^{fl}, n=6 sections from 3 different mice per group); (GCL, ganglion cell layer; INL, inner nuclear layer; ONL, outer nuclear layer)

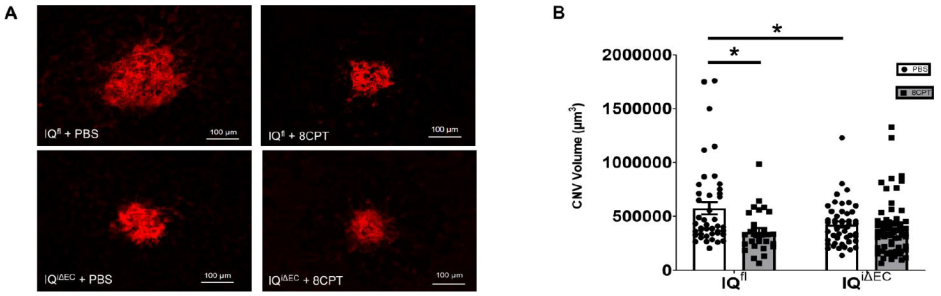

Fig. 8. Activation of Rap1 reduces CNV in the murine laser-induced CNV model by interacting with endothelial IQGAP1.

A) Representative confocal images of lectin-stained RPE/choroid flat mounts from IQ^{fl} and littermate $IQ^{i\Delta EC}$ treated with either intravitreal PBS (first column) or intravitreal 8CPT (second column); B) Quantification of laser-induced CNV volume (Mean±SEM, *$p<0.05$ vs. intravitreal PBS treated IQ^{fl}, n=44 CNV lesions from 11 different IQ^{fl} treated with intravitreal PBS, n=48 CNV lesions from 12 different IQ^{fl} treated with intravitreal 8CPT, n=32 CNV lesions from 8 different $IQ^{i\Delta EC}$ treated with intravitreal PBS, n=56 CNV lesions from 14 different $IQ^{i\Delta EC}$ treated with intravitreal 8CPT)

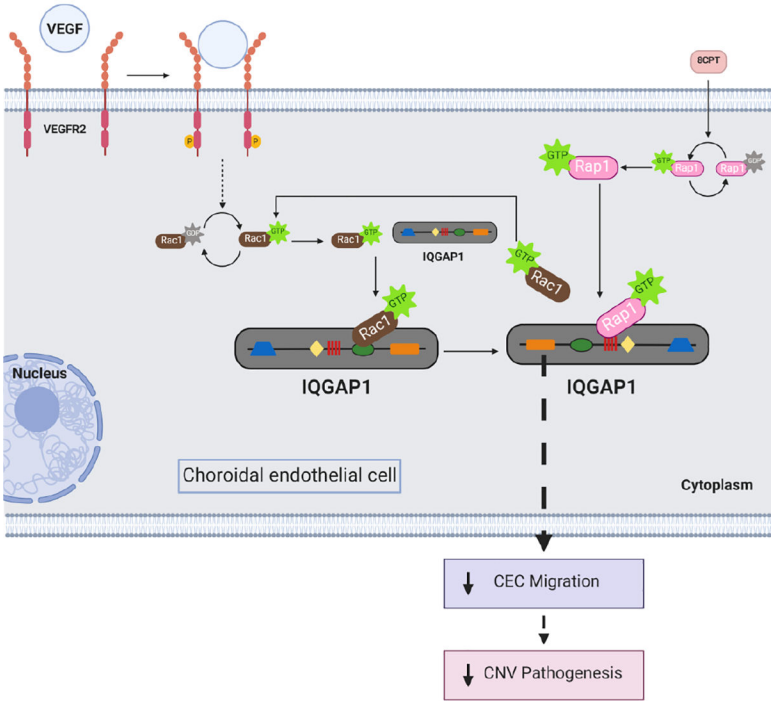

Fig. 9. Diagram of proposed mechanism in which active Rap1 interferes with Rac1 activation.
8CPT-induced active Rap1 binds to the IQ domain of IQGAP1 in choroidal endothelial cells. This interaction between active Rap1 and IQGAP1 interferes with active Rac1 binding to IQGAP1, which prevents sustained Rac1 activation. This results in reduced CEC migration and reduced development of CNV (the diagram was created with BioRender)